COMMISSIONING STATUS OF THE DALIAN COHERNET LIGHT SOURCE

Guanglei Wang for DCLS Commissioning Team[1, 2],
[1]State Key Laboratory of Molecular Reaction Dynamics, Dalian Institute of Chemical Physics, Chinese Academy of Sciences, Dalian, P. R. China
[2]Shanghai Institute of Applied Physics, Chinese Academy of Sciences, Shanghai, P. R. China

Abstract

The Dalian Coherent Light Source (DCLS) is a seeded FEL user facility working at 50-150 nm, now under commissioning in Dalian, China. The facility consists of a 300 MeV normal-conducting S-band linear accelerator (LINAC) and two undulator beamlines. The first beam-line (FEL-1) will provide picosecond FEL radiation with the pulse energy up to hundreds micro-joule, and the second beam-line (FEL-2) will be a femtosecond and polarization controlled FEL. The LINAC and FEL-1 beam-line construction were completed by the summer of 2016, the installation of FEL-2 is in preparation. High power RF conditioning of the LINAC started in August 2016 and the beam commissioning initiated one month later. The saturated HGHG-FEL was obtained in October at the wavelength of 133 nm. This article describes the commissioning status of DCLS, reports on the goals achieved so far.

INTRODUCTION

The DCLS project started in 2012, is designed as a FEL user facility that delivering high quality laser-like photon pulses from 50-150 nm, and will be open to users in the summer of 2017 [1-4]. It's a Linac-based 4th generation light source that operated on the High Gain Harmonic Generation (HGHG) scheme [5-9].The first undulator line, FEL-1, has been successfully commissioned, the FEL-1 could produce picosecond coherent radiation with a tremendously pulse energy for sensitive detection of atoms, molecules and clusters. The second undulator line, FEL-2, will be operated with femtosecond seed laser in elliptical permanent undulator (EPU), then an almighty facility in this wavelength range could be present to serve more scientific application. The main parameters of DCLS are summarized in Table 1.

The civil works were completed by the end of 2015, the LINAC, undulator, and the transfer photon beam line were installed immediately when the building and infra-structure were available. The installation of the facility has been completed in July 2016, and RF conditioning began from August. We started the beam commissioning in the autumn, then successfully generation of 300 MeV electron beam and saturation of FEL amplification, both in SASE and HGHG mode, the saturated FEL gain curve was measured and the pulse energy was over 100 μJ. All essential components of FEL diagnostic area and transport system have also been completed, the user ex-periment will be carried out in the middle of 2017. In this paper, the overview of the DCLS facility and the current status of the FEL commissioning are reported.

Table 1: Design Parameters of the DCLS

Accelerator	
Energy	300MeV
Charge	~0.5 nC
Peak current	300 A
Bunch length	2 ps
Repetition rate	50 Hz
Modulator/Radiator	
Period length	50/30 mm
K-value	1-4/0.5-2.3
Number of periods	20/600
FEL	
wavelength	50-150 nm
Pulse energy	>100μJ

CONFIGURATION OF DCLS

Figure 1 shows the schematic layout of DCLS. The in-jector consists of a 1.6 cell S-band photocathode gun and a 3 m long S-band constant gradient travelling-wave ac-celerator structure (L0). The gun and L0 is fed with a 50 MW Toshiba klystron, about 8 MW to the gun and 25 MW to the L0 in reality. The cathode is developed at Tsinghua University with a 1.5 coupling factor and 14MHz mode separate between the 0 and π mode. The peak field of the gun is about 100 MV/m and the quantum efficiency is over $2x10^{-4}$. When the e-beam is generated from the gun, a focusing solenoid is located immediately downstream for emittance compensation. What's more, a 0.5 m long solenoid is also around the L0 for further beam focusing.

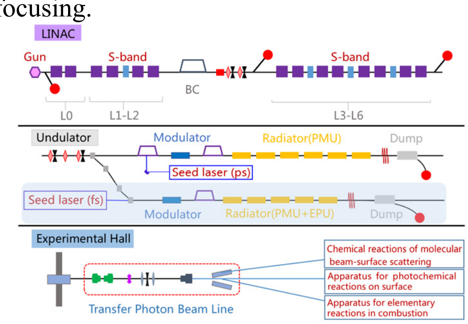

Figure 1: Schmatic layout of Dalian Coherent Light Source.

After the injector, electron beam is accelerated through the S-band linear accelerator. The LINAC is comprised of 6 segments of S-band accelerator structure, each one is 3 m long, and the average accelerating gradient is about 20 MV/m. 3 high power RF stations feed the accelerate structures, the 1st one is 50 MW and the 2nd, 3rd one are 80 MW. Each station serves two S-band units. The pulse length of the high RF power generated by the klystron is

ISBN 978-3-95450-182-3

about 3 µs, the klystrons are operated by modulators with a 200 MW peak power. The beam is accelerated off-crest in L1-L2 to print a radio-frequency-induced curvature, and then is compressed in a movable magnet chicane to improve the peak current. An extra space between L2 and BC is reserved for the X-band linearizer. After the bunch compressor (BC), L3-L6 is located to compensate the energy chirp in upstream and accelerate the beam to the desired energy.

The undulator system is comprised of a modulator, dispersion section and one radiator, the radiator is subdivided into six segments, each 3 m long and with a period length of 30 mm. The modulator gap is variable in order to matching the resonant condition of seed laser at different beam energy, the period length is 50 mm and a total length of 1 m. The energy modulation process are achieved when the electron beam and seed laser are accurately synchronized, both spatially and temporally. Then the dispersion section is introduced to convert the energy modulation into density modulation with a flexible R_{56} from 0 to 0.5 mm. Finally, the micro-bunched beam is sent through the radiator, which is tuned to the *n*th harmonic of the seed wavelength, and coherent FEL radiation at λ/n is emitted. In each break between the undulator, a focusing magnet and a cavity-type electron beam position monitor are mounted on a two-demission movable stage with a preciously control of 10 microns in horizontal and vertical. Besides, a variable-gap phase shifter, composed of four 30 mm magnet pole, is also adopted to exactly adjust the phase between segments so that constructive superposition of the FEL radiation occurs.

Total 19 beam position monitors (BPM) are used for the electron beam position measurements, 10 are cavity BPM which can measure the beam position with sub-micrometer resolution in the undulator beam-line. 3 bunch charge monitors are installed at the exit of gun, LINAC and radiator for the beam loss monitoring. The transverse beam profile is measured by 25 monitors equipped with YAG and OTR screen. What's more, 2 spectrometer dipole systems are located at the gun and BC section, 2 beam dumps at the end of LINAC and undulator, which are utilized for the beam energy measurements.

LINAC COMMISSIONING

At first, to find the designed operating condition of the photocathode gun, we scanned its relative phase with respect to the drive laser, bunch charge was measured as a function of the RF phase. By optimizing the phase of gun and accelerating structures, the strength of solenoids, the laser spot size and pulse length, the injector parameters are finalized. The injector emittance was measured by scanning the twin quadrupole downstream. When a nominal bunch charge to 500 pC is generated, the normalized emittance of injector, as shown in Figure 2, can be optimized to 0.627 and 0.730 mm·mrad in the x and y direction, respectively.

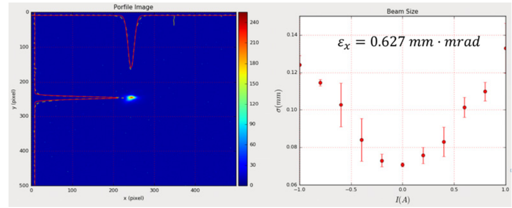

Figure 2: The measurements of the projected emittance by scanning the current of quadrupole. 10 shots were acquired for each quardrupole setting. The RMS value is calculated using the Gaussian fitting. The emittance and twiss parameter results were double checked using both "thin lens" approximation and transport matrix method.

The drive laser for photo-cathode-gun is the third harmonic of a Ti:sapphire laser (~260 nm), with a maximum energy of ~300µJ after the pulse stacking, which is utilized for generating a flat top laser beam. Figure 3 shows the pulse distribution in time domain, the RMS jitter is about 5.6% in the central part, the pulse length is 7 ps FWHM and the laser beam diameter is 2 mm in cathode. Benefit from the high quantum efficiency of the e-gun and sufficient driver laser energy, cathode cleaning is absence in DCLS. In the routinely operation of injector, only 25% of drive laser energy is required for the generation of 500 pC electron beam. The drive laser position, energy and spot size is also monitored by a virtual cathode CCD.

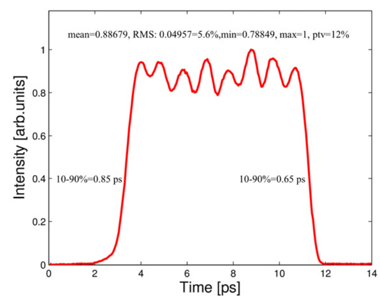

Figure 3: Laser pulse distribution in time domain after the pulse stacking.

To generate a high current beam for the FEL amplification, RF phase of L1-L2 was set to -20° off-crest. The phases of L1-L2 were found by watching the beam distribution at the YAG screen located in the centre of bunch compressor, which is functional as a dipole spectrometer. When the beam is printed a radio-frequency curvature, a horizontally movable chicane is located downstream to compress the bunch length by a factor of ~3. The longitudinal bunch length was measured with a zero-phasing method. The temporal typical profile of the beam is changed into 3.24 ps form the initial 9.63 ps. L3-L4 is operated with a phase of 10° from on-crest for the chirp compensation and L5-L6 is working on-crest. The beam trajectory was adjusted to pass through the centre of the BPM and focusing magnets, by using the magnetic lenses and the steering magnets. The final beam energy was measured to be 312 MeV at the exit of LINAC. With proper optimization of the LINAC, it's possible to obtain a high quality beam with the emittance down to 1.5

mm·mrad, projected energy spread of ~1‰ after compression.

FEL COMMISSIONING

A matching section is inserted between the LIANC and undulator system for beat matching of the designed lattice, and an average beta function of ~10 m is obtained in the undulator. The matching section is composed of 10 quadrupoles which are evenly distributed in the 10 m long free space. After guiding the electron beam to undulator, we performed fine tuning to generate the VUV-FEL. A gas monitor detector and attenuated photodiode are utilized for the observation of FEL pulse energy. The spectrum is measured by a Mcphersion grating spectrometer which is capable of detecting the signal from 30 to 275 nm.

To realize the spatial overlap and relative phase control in FEL amplification process, the beam trajectory along the 20 m long radiator should be aligned with accuracy smaller than 10 μm. General methods, such as beam based alignment are not appropriate in DCLS due to the limitation of beam energy. In order to achieve the optimized trajectory, we optimized SASE first, which is more stringent and sensitive to the beam alignment. Several wavelengths have been carried out in DCLS, including 88, 133 and 145 nm. The wavelength tunability is realized by the variable-gap undulator. On varying the undulator gap from 9-40 mm, a wide tuning range of the deflection parameter K is covered from 2.24 to 0.56. The variable magnet field of radiator enables a rapid and sensitive scan of photon energy. The SASE-FEL is saturated at the wavelength mentioned above, and the corresponding gain curve is measured, the maximum pulse energy achieved so far is about 210 μJ at 133 nm. As mentioned, the absolute pulse energy of DLCS is measured by a photodiode, while the saturation pulse energy of DLCS exceeds 200 μJ, it's too powerful to be detected by a normal photodiode. Therefore, we utilized a metallic mesh with the transmittance of 90% in front of the photodiode, made it sufficient linear in the high intensity region. What's more, the photodiode is also calibrated with the 260 nm drive laser, and according to its QE curve, we calculated the FEL pulse energy with the number read from an oscilloscope.

The HGHG FEL is established when the seed laser is introduced. The transverse overlap of the electron beam and seed laser is achieved by two YAG screen across the modulator, the seed is aligned onto the beam position with two remotely controlled steering mirrors. The seed laser and the spontaneous emission from the modulator are all reflected out the vacuum chamber for temporal overlap. A fast photodiode is located downstream to detect the two signals. The coarse synchronization is adjusted by a phase shifter in timing system, and the fine tuning of arriving time is realized with a delay stage on the seed laser path. In the beginning of HGHG operation, a 266 nm seed laser from the 3rd harmonic of Ti:sapphire system is utilized, the laser pulse energy is of ~170μJ for sufficient energy modulation, and the laser spot size is ~2 mm to maintain a stable transverse overlap. The FEL radiation is maximized by optimizing the resonance condition of the undulator, dispersion strength, and the beam trajectory in the radiator.

The recent FEL performances of HGHG and SASE are summarized in Figure 4. At 133 nm, the FEL saturation output both in SASE and HGHG were realized, as shown in figure 4(a). According to the calibration mentioned above, the pulse energy is 210μJ and 120μJ for SASE and HGHG, respectively. The FEL gain curve along the radiator is also measured and a clearly evidence of FEL saturation can be seen. The obvious stronger of SASE may be caused by the excessive energy modulation in HGHG process, and induced a larger initial energy spread in the FEL amplification. In figure 4(b), the benefit of using external seeding in terms of bandwidth is evidently. The measured bandwidth of SASE is about 1.1 nm (FWHM), and yielding a relative bandwidth of 8.4×10^{-3}, which is comparable to the FEL parameter ρ. For HGHG case, a Gaussian-like spectrum can be observed, the bandwidth is about 2×10^{-3}. The spectrum broadening compared with the Fourier-transform-limited is mainly induced by the residual energy chirp in electron beam and limited resolution of the spectrometer. FEL simulation based on the experimental beam parameters is in good agreement with the experimental results. Once the FEL is working in optimized conditions, its stability could be maintained over a few hours, e.g., the measured intensity jitter is below 20%.

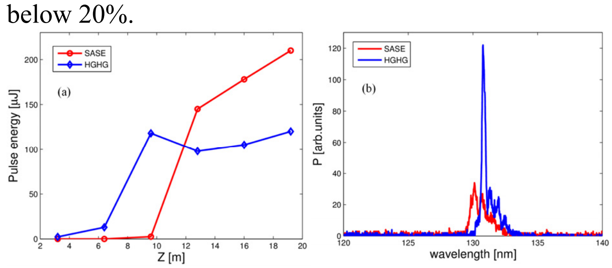

Figure 4: Measured SASE and HGHG performance at 133 nm. a: FEL pulse energy evolution as a function of effective undulator length; b: Comparison of the SASE and HGHG spectrum.

CONCLUSION

The DCLS has been successful commissioned. We attained the full designed performance of the FEL-1 in the October of 2016. The electron beam meets the requirements of stability, energy and project emittance. FEL pulse energy exceeded 100μJ and a saturated gain curve has also been measured in DCLS. First operation with users will be initiated in June 2017. Commissioning of FEL-2 will start at next summer, and complete in the end of 2018.

More detailed optimization of the FEL performance is still required, e.g., commission of the wavelength tuning, tapering experiments, and 50 Hz operation. What's more, some hardware and software upgrading, such as X-band linearizer, transverse deflecting cavity, and more feedback loops are still very necessary in DCLS. All these promotions are already in schedule and will be finished in the next few months.

ISBN 978-3-95450-182-3

REFERENCES

[1] Deng, H.X. et al. Simulation studies on laser pulse stability for Dalian Coherent Light Source. *Chinese Phys. C.* 28, 028101 (2014).

[2] Wang, G.L. et al. Proposal of an X-band linearizer for Dalian Coherent Light Source. MOPOW023, Proceedings of IPAC2016, Busan, Korea.

[3] Zhang, T. et al. FEL polarization control studies on Dalian coherent light source. *Chinese Phys. C.* 37, 118101 (2013).

[4] Wang, G.L. et al. Harmonic lasing options for Dalian Coherent Light Source. MOPOW024, Proceedings of IPAC2016, Busan, Korea.

[5] Yu, L.H. Generation of intense UV radiation by subharmonically seeded single-pass free-electron lasers. *Phys. Rev. A.* 44, 5178-5193 (1991).

[6] Yu, L.H. et al. High-gain harmonic-generation free-electron laser. *Science* 289, 932-934 (2000).

[7] Yu, L.H. et al. First ultraviolet high-gain harmonic-generation free-electron laser. *Phys. Rev. Lett.* 91, 074801 (2003).

[8] Allaria, E. et al. Highly coherent and stable pulses from the FERMI seeded free-electron laser in the extreme ultraviolet. *Nature Photonics*. 6, 699-704 (2012).

[9] Allaria, E. et al. Two-stage seeded soft-X-ray free-free-electron laser. *Nature Photonics*. 7, 913-918 (2013).

ISBN 978-3-95450-182-3